Journal of Thermal Analysis and Calorimetry, Vol. 87 (2007) 3, 703–707

INFLUENCE OF THE SYNTHESIS METHOD ON THE DTG-TPR PROFILES OF Pt/WO_x–ZrO_2 BIFUNCTIONAL CATALYSTS

A. M. Garrido Pedrosa[1*], *M. J. B. Souza*[2], *S. H. Lima*[1], *Dulce M. A. Melo*[1], *A. G. Souza*[3] *and A. S. Araújo*[1]

[1]Federal University of Rio Grande do Norte, Department of Chemistry, CP 1692, 59078-970 Natal-RN, Brazil
[2]Federal University of Sergipe, Department of Chemical Engineering, 49100-000 São Cristovão-SE, Brazil
[3]Federal University of the Paraíba, CCEN, Department of Chemistry, 59059-900 João Pessoa, PB, Brazil

Pt/WO_x–ZrO_2 bifunctional catalysts were synthesized using impregnation and polymeric precursor methods. After the synthesis process the samples were calcined at 600, 700 and 800°C and characterized by X-ray diffraction, nitrogen adsorption and temperature programmed reduction study by thermogravimetry. DTG-TPR profiles showed between three and five reduction events at different temperatures attributed to platinum reduction and to different stages of tungsten species reduction. A comparative study of the synthesis method influence on the DTG-TPR curves was accomplished.

Keywords: *DTG-TPR, impregnation and precursor polymeric methods, Pt/*WO_x*–*ZrO_2

Introduction

Supported tungsten oxide catalysts have been investigated because of their promising application on the isomerization process of *n*-alcanes [1, 2]. A large number of studies concerning the structural feature and active species-support interaction have been performed for WO_x–ZrO_2 catalysts [3–5] and was showed that the active species-support interaction plays an important role in controlling the active phase features and in affecting the support properties. Several works have shown that the catalytic properties of WO_x–ZrO_2 are strongly affected by their synthesis including every step of the preparation together with the quality of precursors and tungsten loading utilized [5–7]. The most widely used method for the preparation of WO_x–ZrO_2 catalysts involves impregnation of precipitated zirconium source with a solution of ammonium metatungstate or paratungstate [1, 6, 7–9]. Other methods have been also used to prepare such oxides, including sol–gel [10], hydrothermal synthesis [11] and using reverse micelles [12]. The preparation of Pt/WO_x–ZrO_2 was not still accomplished by the precursor polymeric method [13] which can be used to prepare catalysts. Such method permits good stoichiometric control as well as reproducibility and yielding ultrafine particles.

The reduction profile of WO_x–ZrO_2 catalysts normally has been studied in the literature for variations in the composition of gas mixture of hydrogen and some inert gas flowing through reactor which are monitored by a thermal conductivity detector (TCD) [14]. The disadvantages this method is the small sensibility of TCD which many times not shown the reduction profile of the components that are in small content in the sample. Compared to that analytical technique of reduction profile study thermogravimetry can provide more accurate information on the metallic sites. In the TG experiments the reduction rate of the several compounds contained in the sample is continuously measured by heating linearly of the material in a reductive gas stream (such as hydrogen). Due to reduction of the different compounds in the sample a variation occurs in the mass of the sample which is monitored by a thermobalance. Different events are related to the species supported and its interaction with the support [15].

This study is focused on the preparation of Pt/WO_x–ZrO_2 catalysts by the impregnation and precursors polymeric methods and on the investigation of the syntheses methods effect on DTG-TPR profiles. X-ray diffraction was used to reveal the structural characteristics of the materials formed.

Experimental

Materials

The Pt/WO_x–ZrO_2 catalysts were synthesized by impregnation (IM) and precursor polymeric (PP) methods using the following chemicals as starting materials: ammonium paratungstate – APT (Aldrich,

---

[*] Author for correspondence: annemgp@yahoo.com

1388–6150/$20.00

Akadémiai Kiadó, Budapest, Hungary
Springer, Dordrecht, The Netherlands

99.99%), zirconium oxonitrate (Aldrich) and platinum(II) chloride (Aldrich, 99.9%). These reactants were combined to obtain samples contain 1 mass% of platinum and 10, 15 and 20 mass% of tungsten after calcination treatments.

Impregnation method (IM)

$Pt/WO_x–ZrO_2$ catalysts were prepared by success impregnation of the tungsten and platinum precursors on source of support with basis on the method proposed by Hino *et al*. [1, 4]. In this procedure the preparation of aqueous solutions of ammonium paratungstate is going at first. These solutions were added to the zirconium source solids with stirring at 70–80°C for 1 h. After then platinum chloride solutions were added to the systems mentioned above in appropriate amount. The resulted solutions were kept at that temperature for 4 h resulting in precursor powders.

Precursor polymeric method (PP)

The procedure to obtain $Pt/WO_x–ZrO_2$ catalysts were: (*i*) stoichiometric amounts of ammonium paratungstate and distilled water were placed to Beckers and stirred at 50–60°C for 30 min; (*ii*) an aqueous solution of citric acid (Vetec) and stoichiometric amounts of zirconium oxonitrate were mixed at 60–70°C for 1 h. The molar ratio between citric acid and zircon was of 2:1; (*iii*) the solution (*i*) was added to the solution (*ii*) under constant magnetic stirring and kept at 70°C for 30 min; (*iv*) stoichiometric content of platinum chloride solid was then added to the system (*iii*) and stirred at 70°C for period less than 10 min; (*v*) after complete mixing, the temperature was slowly increased to 90°C at which point ethylene glycol (Vetec) was added with the mass proportion of 60:40 (citric acid: ethylene glycol). The resulted solution was held at that temperature for 1 h under constant magnetic stirring. A gel was then formed and subsequently heat-treated at 300°C for 2 h resulting the precursor powders.

Methods

The materials obtained in both synthesis processes were denominated of PWZ10, PWZ15 and PWZ20. These materials were calcined at 600, 700 and 800°C for 1 h. The identification of the crystalline phases formed after calcination process were performed by X-ray diffraction in a Shimadzu (XRD-6000) equipment using Ni-filter and CuK_α radiation, with diffraction angle (2θ) in the range of 10–80°.

Thermal stability of the calcined samples were investigated by heating of 3 mg of each sample using Shimadzu TGA-50 instrument at a heating rate of 10°C min^{-1} under air (flow rate: 50 cm^3 min^{-1}). The catalysts were characterized by temperature programmed reduction (TPR). The procedure consisted in activating the sample at 100°C for 30 min in nitrogen flow. After this treatment, the TPR profile was performed by heating of about 30 mg of sample from 100 to 900°C in a Mettler TGA-851 instrument at a heating rate of 20°C min^{-1} and under hydrogen purging at a flow rate of 25 cm^3 min^{-1} ion alumina crucible. The hydrogen consumption was measured by thermobalance.

Results and discussion

Calcinations at 600, 700 and 800°C lead to removal of physically adsorbed water, decomposition of precursor, as well as condensation of tungstate species on zircon surface. In the case of $Pt/WO_x–ZrO_2$, the calcination process can also lead to the formation of acid sites as a result of adsorption of tungstate species on support creating Brönsted-type acidic sites. TG/DTG curves of the calcined samples (figure not shown) revealed 0.5–1.5% mass loss (for the samples prepared by IM method) and 1–4% (for the samples prepared by PP method) in the temperature range of 30–600°C. The observed mass change probably related to the decomposition of the hydroxyl groups. Such results suggest that the synthesis methods used were effective for complete decomposition of the precursors as well as to obtain the final catalysts.

Crystalline phases were obtained by calcinations between 600 and 800°C as suggested by the presence of strong peaks. X-ray diffractograms of the $Pt/WO_x–ZrO_2$ materials calcined at 700°C are shown in Figs 1a and b for the samples prepared by IM and PP methods, respectively. For the samples prepared by IM method, the diffractograms showed the main peaks of monoclinic (m) and tetragonal (t) phases of zircon oxide (ZrO_2) with 2θ=28.2° (m); 30.2° (t) and 31.3° (m) and monoclinic phase of tungsten oxide (WO_3). Other peaks relative to zircon oxide also were observed but they are overlap with the WO_3 oxide. WO_3 oxide only was observed in the samples containing more than 10% of tungsten (PWZ15 and PWZ20). This structure was characterized in the samples by peaks with 2θ=23.1, 23.6 and 24.3°. In case of the samples prepared by PP method, the diffractogram showed the main peaks of tetragonal (t) phase of zircon oxide (ZrO_2) with 2θ=30.2° (t), 35.2° (t), 50.3° (t) and 60.1° (t). Some samples shown peaks due monoclinic (m) phase of zircon oxide (m-ZrO_2) and due a monoclinic phase of tungsten oxide (WO_3). The principal peaks due m-ZrO_2 was at 2θ=28.2, 31.4 and 55.6°. WO_3 phase was observed in the PWZ20 sample calcined at 700°C, PWZ15 and PWZ20 calcined at 800°C. The presence of platinum on tung-

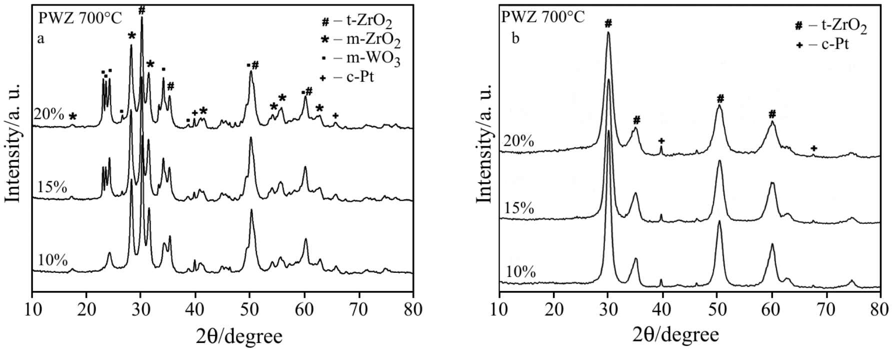

Fig. 1 XRD of Pt/WO$_x$–ZrO$_2$ samples prepared by a – IM and b – PP methods, with different tungsten load (10, 15 and 20%) and calcined at 700°C

sten-zircon oxide (WO$_x$–ZrO$_2$) phase was observed in all samples independent of the synthesis method and even platinum is in small contents on surface of the catalysts. In these samples the platinum crystalline phase was identified by two main peaks at 2θ equal to 39.8 and 65.6°. The presence of platinum metallic species was also previously found in other works when the platinum was added before calcination [6]. Comeli *et al*. [16] studied and concluded that tungsten induces electronic and/or steric modifications upon Pt particles in Pt/WO$_x$–ZrO$_2$ type materials.

TPR-DTG curve of bulk WO$_3$ crystallites calcined at 700°C (figure not shown) exhibited a shoulder and two reduction peaks with maxima at 650, 748 and 870°C. These reduction peaks are related to the reduction of WO$_3$ and of its formed species. The first reduction peak begins at 630°C with the partial reduction of WO$_3$ forming non-stoichiometric (WO$_{2.9}$) tungsten oxide intermediate. At approximately 685°C the simultaneous reduction of this oxide and of WO$_3$ takes place, then the reduction of these oxides resulting in the WO$_2$ species is going on. The reduction of WO$_2$ begins at 791°C forming metallic tungsten (W^0). This last reduction peak was not completed under the applied experimental conditions. Similar results were also observed by Vaudagna [6].

DTG curves recorded during the hydrogen consumption of Pt/WO$_x$–ZrO$_2$ and with different tungsten loading and calcined at different temperatures are shown in Figs 2–4. These curves were denominated of temperature programmed reduction by thermogravimetric analysis (TPR-DTG). In agreement with the DTG curves (Figs 2–4) three–four main mass loss events for the samples prepared by IM method (figures on the left side) and three–five main mass loss events for the samples prepared by PP method (figures on the right side) were identified. For the samples prepared by IM method, TPR-DTG profile showed a reduction peak, which is not well defined at low temperatures (~150°C) which can be related to the platinum oxide reduction [6]. The low temperature for platinum reduction can be correlated with a low interaction between platinum oxide species and the supporter. For the samples prepared by PP method, TPR-DTG curves showed two reduction peaks at 137 and 230°C which are probably related to the reduction of Pt^{4+} to Pt^{2+} and the second peaks due the reduction of Pt^{2+} to Pt^0. In accordance with XRD results a part of platinum deposited in the supporter during the synthesis was reduced and after calcinations platinum metallic deposited on the support were obtained. The same behavior was also observed in other works when the platinum was added before calcination [6]. Therefore the peak appeared at ~150°C (for the samples prepared by IM method), and at 137 and 230°C (for the samples prepared by PP method) are due the reduction of platinum oxide species remainder the synthesis process.

TPR-DTG profile for the samples prepared by IM method also showed three–four overlapping reduction peaks which are related to the WO$_x$ reduction. In the samples contain 10% of tungsten (PWZ10) and calcined at different temperatures, XRD results not indicated the presence of WO$_3$ crystalline structure. On the basis of these results we assumed that the two peaks showed at 670 and 720°C in these samples can be attributed to reduction of WO$_x$ species (amorphous and non-stoichiometric oxides). In this case the tungsten is in octahedral and tetrahedral coordination and the two peaks are corresponding to the reduction of non-stoichiometric oxides to metal tungsten which occurs in two steps. The samples containing 15 and 20% of tungsten (PWZ15 and PWZ20) calcined at 600°C exhibited similar behavior. In these samples XRD results showed the presence of WO$_3$ crystalline structure. TPR-DTG profile for these samples showed two broad peaks which correspond to several overlapping reduction steps. TPR-DTG profile for the samples prepared by PP method also showed three–four overlapping reduction peaks which are totally different of the profile of pure WO$_3$. This suggests that the tungsten species supported are not mainly composed of WO$_3$ species. Such curves exhibited a large reduction peak to high temperatures with a maximum in the 760–860°C tem-

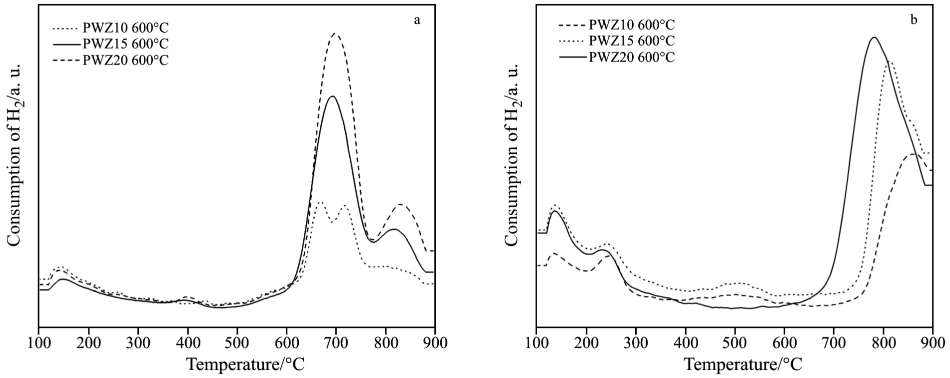

Fig. 2 TPR-DTG profiles of Pt/WO_x–ZrO_2 samples prepared by a – IM and b – PP methods with different tungsten load (10, 15 and 20%) and calcined at 600°C

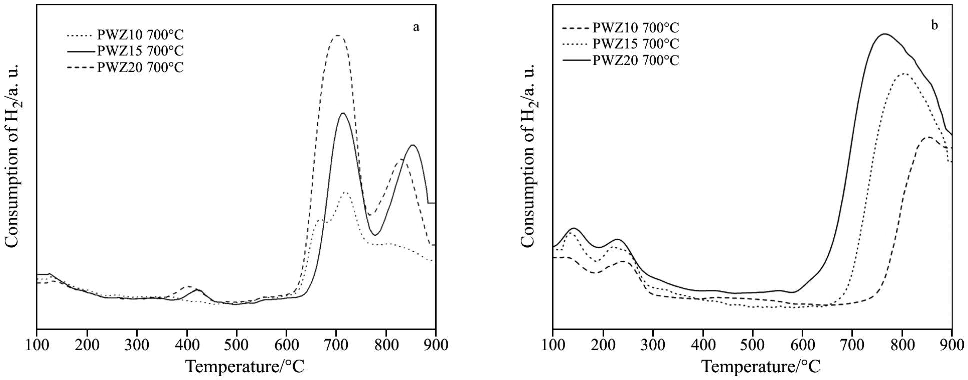

Fig. 3 TPR-DTG profiles of Pt/WO_x–ZrO_2 samples prepared by a – IM and b – PP methods with different tungsten load (10, 15 and 20%) and calcined at 700°C

perature range, which is related to the reduction of the amorphous tungsten oxides anchored to the zirconium oxide. In this case the tungsten is in octahedral and tetrahedral coordination and it can contain W^{6+} and W^{5+}. Although the reduction of the tungsten species in the octahedral coordination takes place at lower temperatures than the species in the tetrahedral coordination, in the case of these samples (figures on the right side) several simultaneous and parallel reactions should be take place. Reduction peaks due WO_3 crystallites were not observed in the samples that exhibited this phase in the XRD patterns. This observation can probably be the result of the reduction of these crystallites which happens simultaneously with the reduction of WO_x species. The PWZ sample calcined at 800°C exhibited a peak splitting at high temperatures, which can be related to a better dispersion of the octahedral and tetrahedral species. In addition, this sample show a reduction peak at 423°C which can be related to the reduction of WO_3 crystallites.

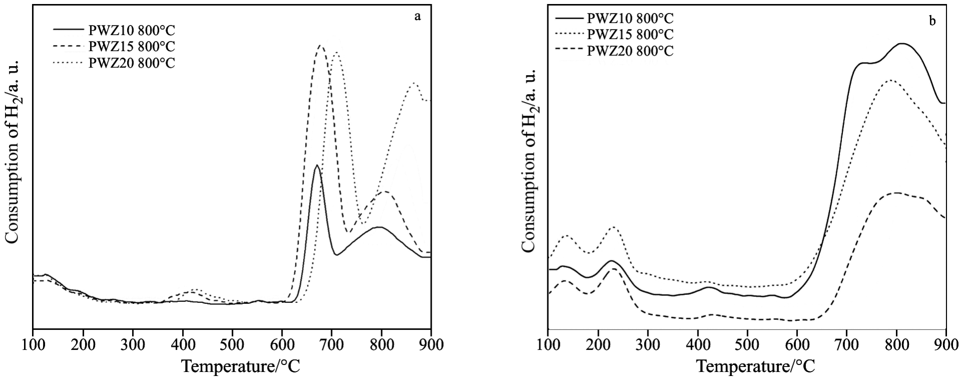

Fig. 4 TPR-DTG profiles of Pt/WO_x–ZrO_2 samples prepared by a – IM and b – PP methods with different tungsten load (10, 15 and 20%) and calcined at 800°C

The effect of calcination temperature on the reduction profile of several Pt/WO_x–ZrO_2 samples can also be seen in Figs 2–4. For the samples prepared by IM method with the increase of calcination temperature the platinum reduction peak practically disappears.

This can be related to an extensive platinum sinterization or with the formation of mixed metal or yet with the formation of metal oxide clusters [6, 16]. On the other hand with the increase of calcination temperature we also observed the appearance of a peak between 350–450°C in the samples containing 15 and 20% of tungsten (PWZ15 and PWZ20). The appearance of this peak can be related to the WO_3 crystallites which only were detected in the samples contain 15 and 20% of tungsten. In this case we can attribute this peak at catalytic action of the platinum on tungsten species reduction [6, 16]. Therefore, we can conclude that in the PWZ15 and PWZ20 samples calcined at 700 and 800°C the peak appeared at 350–450°C is attributed to the first step of WO_3 reduction ($WO_3 \rightarrow WO_{2.9}$). The broad and intense peak at 700°C is attributed to the second reduction step of WO_3 crystallites ($WO_{2.9} \rightarrow WO_2$) and to the beginning of the reduction of WO_x species. The third reduction peak which can be seen approximately at 830°C can be attributed to the third reduction step of WO_3 crystallites ($WO_2 \rightarrow W$) and to the second step of WO_x resulting metal tungsten species.

Conclusions

Crystallization of Pt/WO_x–ZrO_2 occurs upon calcination. Both synthesis methods are going with the formation of Pt/WO_x–ZrO_2 catalysts resulting differences phases. Due to the ZrO_2 (tetragonal) and platinum metallic phases, all Pt/WO_x–ZrO_2 samples showed peaks in the XRD diffractograms upon calcination at 600, 700 and 800°C. The WO_3 and ZrO_2 (monoclinic) phases were observed only in some samples. The syntheses methods, the calcination treatments and the tungsten load have influence on the reduction profile of Pt/WO_x–ZrO_2 catalysts. TPR profiles showed three–five events at different temperatures which are attributed to platinum reduction and the different stages of tungsten oxide reduction.

Acknowledgements

The authors acknowledge the Agência Nacional do Petróleo (PRH/ANP 30) and to the CNPq.

References

1 M. Hino and K. J. Arata, J. Chem. Soc.-Chem. Commun., 18 (1988) 1259.
2 Y. Ono, Catal. Today, 81 (2003) 3.
3 D. G. Barton, S. L. Soled, G. D. Meitzner, G. A. Fuentes and E. Iglesia, J. Catal., 181 (1999) 57.
4 K. Arata and M. Hino, Mater. Chem. Phys., 26 (1990) 213.
5 M. Valigi, D. Gazzoli, I. Pettiti, G. Maattei, S. Colonna, S. Rossi and G. Ferraris, Appl. Catal. A Gen., 231 (2002) 159.
6 S. R. Vaudagna, R. A. Comeli and N. S. Figoli, Appl. Catal. A Gen., 164 (1997) 265.
7 M. G. Falco, S. A. Canavese and N. S. Figoli, Catal. Today, 107–108 (2005) 778.
8 J. G. Santiesteban, J. C. Vartuli, S. Han, R. D. Bastian and C. D. Chang, J. Catal., 168 (1997) 431.
9 F. D. Gregorio and V. Keller, J. Catal., 225 (2004) 45.
10 O. V. Melezhyk, S. V. Prudius and V. V Brei, Micropor. Mesopor. Mater., 49 (2001) 39.
11 E. Tani, M. Yoshimura and S. Somiya, J. Am. Ceram., 66 (1983) 11.
12 W. Sun, L. Xu, Y. Chu and W. Shi, J. Colloid Interf. Sci., 266 (2003) 99.
13 P. A. Lessing, Ceram. Bull., 68 (1989) 1002.
14 M. Afzal, G. Yasmeen, M. Saleem and J. Afzal, J. Therm. Anal. Cal., 62 (2000) 277.
15 A. M. Garrido Pedrosa, M. J. B. Souza, D. M. A. Melo, A. G. Souza and A. S. Araujo, J. Therm. Anal. Cal., 79 (2005) 439.
16 R. A. Comelli, Z. R. Finelli, S. R. Vaudagna and N. S. Figoli, Catal. Lett., 45 (1997) 222.

DOI: 10.1007/s10973-006-7777-x